The Practical Design of In-vehicle Telematics Device with GPS and MEMS Accelerometers

Milan B. Vukajlović, Srdjan Tadić, and Dejan M. Dramićanin

***Abstract* — The latest generation of vehicle tracking devices relies not only on Global Positioning System (GPS) but also uses low-cost Micro-Electro-Mechanical Systems (MEMS) accelerometers. This combination supports new services such as driving style characterization and Automatic Crash Notification (ACN). Our focus will be on practical considerations of such a telematics unit. The paper will consider the boundaries of allowed errors and minimal requirements for sensors and mounting requirements. Sensor range for crash detection and impact angle estimation was tested on field trials with two units containing accelerometers range of 18g and 2g. The kinematic orientation of vehicle is evaluated in a series of field trials with a resulting standard deviation of estimation of 1.67°. The second run of experiments considers the dynamic range and sampling rate of sensors during collision. A sensor range of 8g (typical for present-day telematics devices) can be used to detect crash without accurate knowledge of impact angle.**

***Keywords* — Accelerometer, advanced vehicle tracking, automatic crash notification, GPS, telematics.**

I. INTRODUCTION

GPS tracking devices and event data recorders (EDR) are common equipment in modern vehicles, either as a part of embedded car electronics or as "aftermarket" devices installed to support various telematics services. Evolution of modern fleet management tools brings a wider span of supported services. Common examples are characterization of driver behavior and automatic crash notification. This is followed by an increase of processing power available on board and introduction of MEMS motion sensors. Telematics services today are commonly based on "aftermarket" tracking units that are built-in after purchase of the vehicle. This is partly caused by flexibility reasons. The backbone of information infrastructure are GPRS links and "cloud computing". GPS and motion sensors are often combined with data coming from a vehicle On-Board-Diagnostics (OBD) bus. This redundancy makes speed information more reliable. Current trends show a need for a deeper analysis of driver behavior and recognition of undesired driving patterns. Devices are becoming a step closer to GPS/INS navigation systems.

Being "aftermarket" is usually a drawback for devices with accelerometers. Such devices always need rigid and precise mounting. Vibrations or improper axis alignment affects data integrity. Hence, device installation is a critical operation considering reliability/repeatability, time consumption and cost. Optimization of this process would bring large benefits to service suppliers.

Complex and fatal crashes are often a matter of dispute in forensic investigation because existing tools provide only lines of march and demand a high level of expertise to resolve ambiguities. This paper will consider technical requirements for measuring specific forces in a vehicle during crash that would provide accurate characterization of crash severity – such as sensor dynamic range, resolution and sampling rate regarding real-vehicle physics validated on field trials.

Milan B. Vukajlović, Bitgear, Generala Mihajla Nedeljkovića 12, 11000 Belgrade, Serbia (e-mail: milanvukajlovic86@gmail.com).

Srdjan Tadić, Bitgear, Generala Mihajla Nedeljkovića 12, 11000 Belgrade, Serbia (e-mail: srdjan.tadic@gmail.com).

Dejan M. Dramićanin, Bitgear, Generala Mihajla Nedeljkovića 12, 11000 Belgrade, Serbia (e-mail: dejan.dramicanin@gmail.com).

II. LEVELING AND FINDING DEVICE ORIENTATION

A. Device Leveling

The accelerometer measures *specific* forces in a sensor "body" coordinate frame, which in general differs from a vehicle coordinate frame. An application like this usually requires a simple horizontal leveling procedure. One option is to measure gravity components while a vehicle is stationary and o a flat surface [1]. This provides two out of three Euler angles required to estimate the initial Transformation Cosine Matrix. The Transformation Cosine Matrix can be defined considering three successive rotations of angles φ (roll), θ (pitch) and ψ (yaw) around the *x*, *y* and *z* axis respectively (Fig. 1). It is a link between acceleration in "vehicle" and "body" coordinate frame (1).

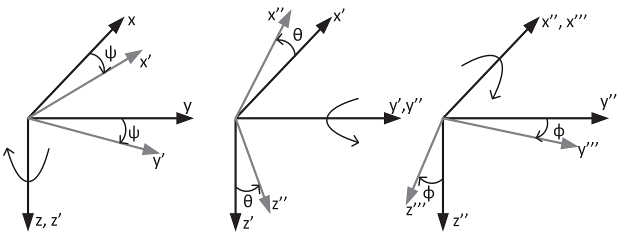

Fig. 1. Euler angles.

$$\begin{bmatrix} a_x^v \\ a_y^v \\ a_z^v \end{bmatrix} = \begin{bmatrix} \cos\psi\cos\theta & -\sin\psi\cos\phi + \cos\psi\sin\theta\sin\phi & \sin\psi\sin\phi + \cos\psi\sin\theta\cos\phi \\ \sin\psi\cos\theta & \cos\psi\cos\phi + \sin\psi\sin\theta\sin\phi & -\cos\psi\sin\phi + \sin\psi\sin\theta\cos\phi \\ -\sin\theta & \cos\theta\sin\phi & \cos\theta\cos\phi \end{bmatrix} \begin{bmatrix} a_x^b \\ a_y^b \\ a_z^b \end{bmatrix} \quad (1)$$

The lower boundary of accelerometer resolution (sensitivity) depends on allowed leveling and orientation error. Rough installation introduces leakage of specific forces to other axis which increases a chance of false-alarming. Undesired components should be kept at least one order of magnitude lower than forces typical for listed driving events. The rule-of-thumb for this application is to enable leveling within 1-2 degrees that should be achievable with sensor sensitivity in the order of 10-20mg.

At consumer/automotive grades of sensors there is also a significant influence of imperfections of MEMS technology on leveling accuracy [2]. Dominant is the effect of zero-G bias, which at this grade might be on a level of 20mg. Sensor temperature variation is usually almost one order of magnitude lower over the whole temperature span of interest. A significant source of error might also be the physical non-orthogonality of sensor axis which is above 1% for this type of IC's. Leveling is usually less sensitive to other usually modeled errors such as a scale factor and nonlinearity. These effects come to importance in high dynamic environment and will more affect reliability while extracting crash angles. A cumulative effect might degrade leveling accuracy. Though, forces present at vehicle during typical driving provide a certain level of robustness when using such devices for driving behavior analysis. As a consequence, in practice, it is not usually necessary to do specific calibration. Device leveling is done in a real time. Angles are recalculated only if vehicle is stationary.

B. Orientation Algorithm

The GPS provides vehicle heading at 1s time instants. In general this orientation is not the same as for device. One approach to override rigid and time consuming measuring of device orientation is to incorporate a filter for kinematic alignment [3]-[5]. Kinematic alignment relies on external speed and acceleration sources such as GPS or odometer, and external heading info as from GPS or a magnetic sensor. Kinematic alignment algorithms use external heading information to estimate yaw angle. GPS heading is used in the algorithm instead of magnetic sensor heading because of indispensable magnetic sensor calibration and the influence of uncorrelated magnetic disturbances caused in the proximity of metal and magnets on sensor output [6], [7]. Hence, the kinematic alignment method with GPS heading, odometer data and three-axis accelerometer is tested. Device orientation relative to vehicle is recursively estimated in real time while vehicle is accelerating or braking with a constant direction. A constant direction is detected according to GPS heading data (2), where V_E and V_N are speed components in east and north directions. GPS receiver uses knowledge of the components of speed directed to north and east to find heading. By elementary math, heading is less accurate at low speeds or while driving along North or East. These cases should be filtered out as outliers. Another fact is that GPS data are always delayed regarding inertial data. Delay is usually greater than half a second. When vehicle is turning the effect is harmful. A simple filter would be to search only for intervals with a constant GPS heading for at least 3 seconds. This excludes potential start of cornering in latter second. Accelerations a_y and a_x (3) are mean values from a previous second. Precise device orientation is possible only if these components have a notable value. Hence, two conditions should be met for kinematic orientation in this simple way – a certain level of acceleration and a constant heading.

Algorithm 1 - Simple Kinematic Alignment

```
while 1 do
if (|V_N| > THR_SPEED && |V_E| > THR_SPEED)
    if heading_gps(t) = heading_gps(t-1s)
        cnt++;
        if ((cnt>3) and (speed(t-1s)– speed(t-2s)>THR))
            heading = -atan(a_y(t-1s)/a_x(t-1s));
        end
    else
        cnt = 0;
    end
else
    cnt = 0;
end
end while
```

$$H^{GPS} = \arctan\left(\frac{V_E^{GPS}}{V_N^{GPS}}\right) \tag{2}$$

$$\psi = -\arctan\left(\frac{a_y}{a_x}\right) \tag{3}$$

C. Field Trials

A passenger car was equipped with a GPS tracking unit with consumer grade MEMS accelerometers. Two 20-minute rides were logged under regular driving conditions in urban environment (Fig. 2). Initial roll (-0.4˚) and pitch (4.1˚) angles were calculated after mounting. According to the photo of mounted device (Fig. 3), a relative angle between device and vehicle longitudinal axes ("box orientation") was approximately 68˚.

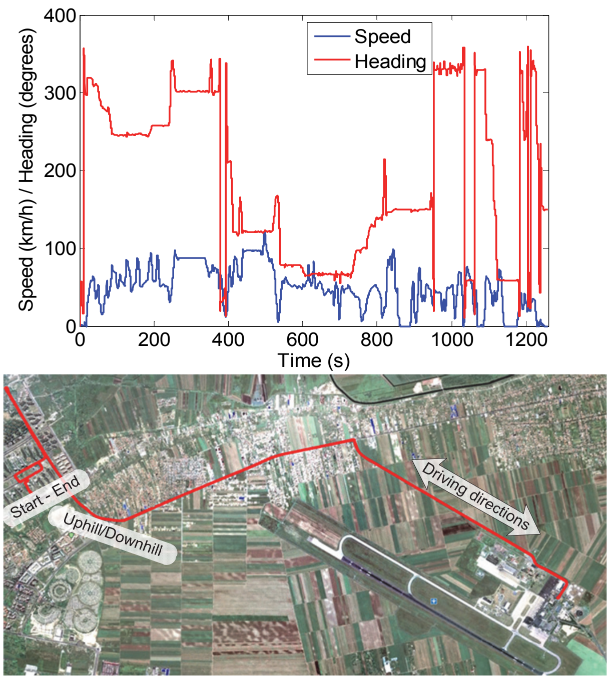

Fig. 2. Speed, heading and route of the first of test drives.

The emphasis of tests was on device orientation. By the proposed method, orientation angle should slowly converge to an acceptable value. In reality, convergence time might be even measured in days after device installation. Calculation is affected by misalignment between the sensor, printed circuit board and enclosure, as well as with the built-in non-orthogonality of sensor axes. These effects could not be measured by photo or mechanical tools. As after effect, the overall deviation of "true" orientation from assumed value might be roughly up to ±5˚.

Fig. 4 shows results of the first trial. Speed difference threshold in this run was set to 1.9m/s, and calculated yaw angle was 67.33˚. The standard deviation of 18 obtained results was 1.67˚. By lowering the threshold which is dual to increasing the filter bandwidth, the number of available estimations will rise. Experiments show that an increased number of measurements will not compensate a higher level of noise introduced to algorithm, resulting in worsening standard deviation.

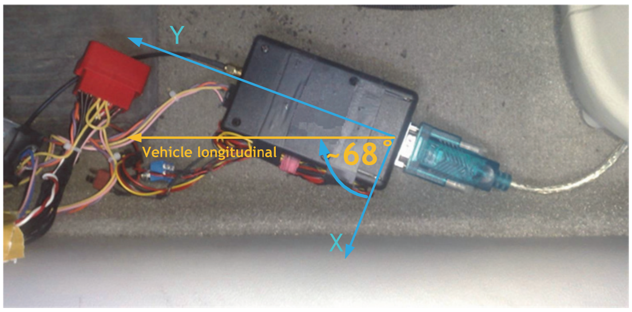

Fig. 3. Car-mounted telematics unit.

Fig. 5 illustrates results obtained on the same run with lower thresholds of 1.5m/s. Now, the number of yaw angle estimations rises to 25, but this benefit was poorly traded with an increased standard deviation of 4.6˚.

Suitable calculation intervals depend on individual driving patterns. Still, as a general rule, it has been identified that acceleration sections which satisfy all conditions were much less frequent. These sections were also less noisy and the standard deviation of estimations done on these intervals was significantly lower than on braking sections (2.44˚ compared to 1˚ on some tests).

The second trial illustrates a possible drawback of this simple approach. Specific traffic conditions allowed only one estimate of yaw angle (72˚) in a 20-minute period.

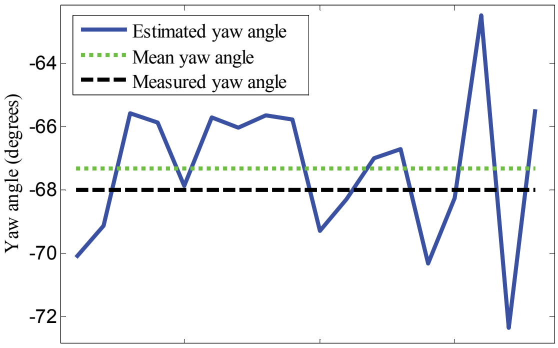

Fig. 4. Yaw angle estimations – rigid thresholds.

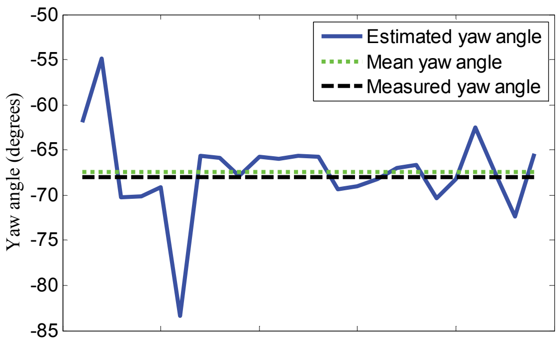

Fig. 5. Yaw angle estimations – lower thresholds.

Road-traffic jam limited car dynamics and recorded accelerations/brakings exceeded pre-defined thresholds at only one point of journey. Other tests in regular driving conditions and on various terrains and road inclinations confirmed a very similar level of standard deviation of measurements.

The aim of the next experiment was to answer if this level of orientation error is acceptable for *driving style characterization*. The answer depends on the magnitude of specific forces typically measured during targeted driving events. As an example, similar setup recorded the lateral acceleration of car while cornering at high speed with a small radius of curvature (Fig. 6). Recorded data were post-processed in simulation to add the effect of yaw angle error of 5˚. Simulation has verified that error is one order of magnitude below specific forces of interest. The lateral acceleration threshold was preset to 6m/s^2, while acceleration error (Fig. 7) was below 0.4m/s^2. It can be assumed that influence on false detection of a cornering event is limited and acceptable.

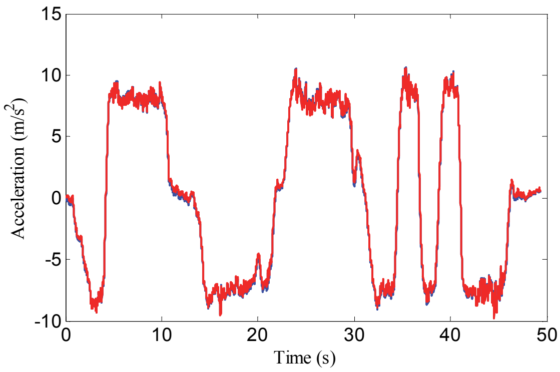

Fig. 6. Real lateral acceleration and simulated contribution of yaw angle error of 5˚.

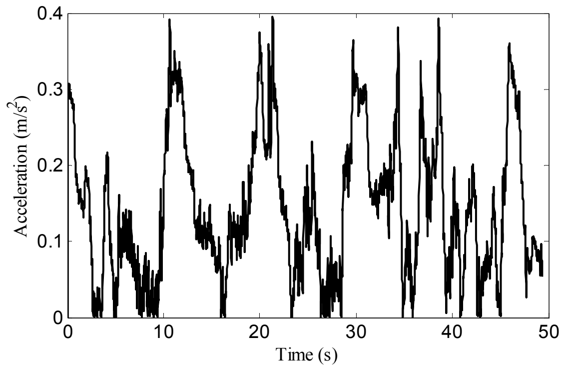

Fig. 7. Difference between real lateral acceleration and simulated contribution of yaw angle error of 5˚.

III. Crash Detection Requirements

A. Required Sensor Parameters

ACN is an important component of modern and future telematics services. It is important to consider minimal technical requirements of GPS and sensors.

The duration of "typical" vehicle crash almost never exceeds 300ms [8]. The highest level of energy exchange during a typical crash is usually within starting 50ms. Following this, the accelerometer sampling rate roughly should be at least 50-100Hz. This exceeds the rate required for driving style characterization. It also makes GPS useful only during pre- and post-crash intervals.

Severe crashes may reach levels of up to 50-100g's depending on conditions [8]. In the USA, federal regulations [9] define minimal specifications of EDR sensor if it was embedded in a vehicle in production and for the purpose of crash recording (Table 1). These standards are not obligatory for aftermarket devices. Most of the aftermarket devices that are currently present in vehicles do not match these criteria. Usually, they cover a range of 4-10g. In case of crash, output is saturated. Override of this problem could enable ACN on many already produced devices.

TABLE 1: EDR ACCELEROMETER REQUIREMENTS (USA).

Acceleration	Min. range	Sensitivity	Sampling rate
Lateral	±5 g	0.5 g	100 Hz
Longitudinal	±50 g	0.5 g	100 Hz
Normal	±5 g	0.5 g	100 Hz

B. Crash Test Setup

Crash is a complex and non-linear event. One possible approach to analysis is field testing. Concerning practical reasons, a 1:5 scaled down and reinforced model car was used for a crash test. The test was prepared considering mechanical aspects such as weight, ratio of tire size and surface fairness, engine vibrations and suspension. Two inertial measurement units were used. The first unit covered a 2g dynamic range at a rate of 100Hz with 18mg/LSB resolution. This device represented consumer grade technology that is common for already deployed devices. The second, referent, device covered a wider dynamic range of 18g, at a sampling rate of 200Hz and with a sensitivity of 3.33mg/LSB. A referent device was industry grade IMU but this fact is not prevailing for this type of crash analysis due to high dynamics and short intervals of interest. Data were recorded in a flash memory and post-processed in MATLAB as shown on a block diagram in Fig. 8.

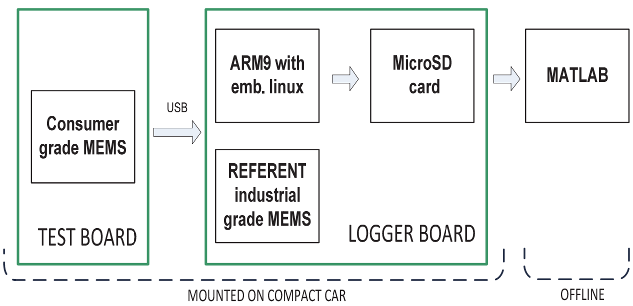

Fig. 8. Block diagram of crash-test setup.

C. Test Scenario

The device recorded a full frontal crash of a compact car into a barrier. A cardboard box with partially homogeneous content has served as a barrier. The box weighed app. 10kg that was similar to the weight of a model car. A barrier was placed on a concrete surface with low friction in between. A barrier was supported by a metal bar placed on lower back side.

Impact speed was approximately 30kmph ("event 1"). A hit caused box rotation around the axis that coincides with a metal bar. Moderate deformation of box combined with its rotation brought to the rotation of model car around a mirrored axis positioned on car lower back side. Car reared to an angle between 45˚ and 90˚, and returned to a previous horizontal position ("event 2"). Movement continued until the final impact to a metal bar (full frontal) at low speed ("event 3"). Fig. 9 shows video snapshots of this event.

This simple test comprised multiple crash events with various obstacles. Scope was on crash detection and angle of impact, commonly known as Principal Direction of Force (PDOF). PDOF is very valuable to an expert-witness.

Referent and tested device outputs are shown in Fig. 10 and Fig. 11 respectively. A change of speed vector is normalized by predefined law.

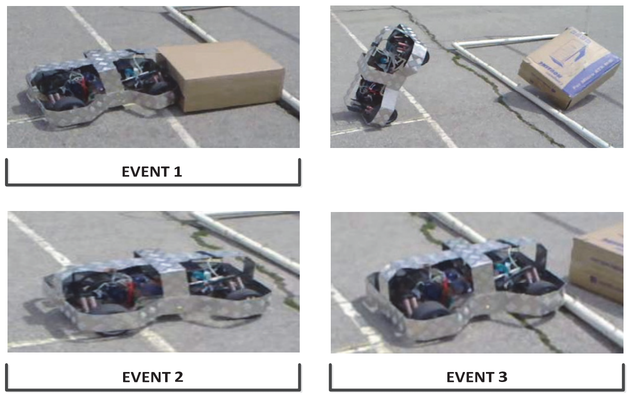

Fig. 9. Snapshots of crash test video.

A referent unit successfully detected crash events while a tested unit detected only the strongest one. According to the value of normalized delta-V, all three axes on a tested device should be saturated to detect a crash of this severity. This means that crash events aligned with any device axis could not be detected.

Crash PDOF should be calculated at the moment of detection. The peak value of delta-V thus does not have to be crucial for its calculation. The next question is whether it is possible to get a fair estimate of PDOF if sensor were saturated. The assumed "true" value of PDOF was app. 10˚ in a horizontal and -5˚ in a vertical plane. A referent device calculated (17˚h, -8˚v). Tested device PDOF output was (47˚h, 23˚v) which is only sub-quadrant precision. Referent sensor data were degraded in MATLAB environment to match tested data and obtained results are shown in Table 2. Test verifies that PDOF accuracy is severely degraded even if sensors are being saturated at much higher values or while operating on a higher rate.

One possible approach to partly override saturation is to use polynomial interpolation techniques. Cubic spline approximation is used for data reconstruction (4) – (8) with *h* as duration of sensor clipping.

Approximation enabled detection of all events, but was not able to recover PDOF (43˚h, -61˚v) (Fig. 12). Polynomial interpolation effects maximal acceleration on low sampling rates.

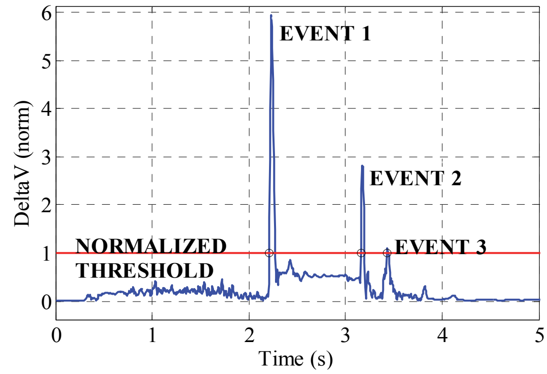

Fig. 10. Referent device normalized delta-V.

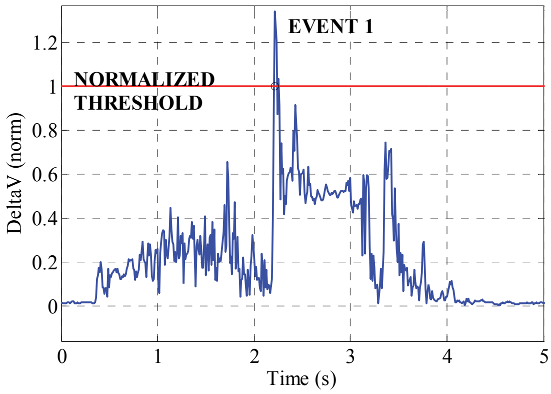

Fig. 11. Tested device normalized delta-V.

TABLE 2: RESULTS OF PDOF CALCULATIONS.

Data	Dynamic range	Sampling rate	Horiz. angle	Vertical angle
Referent	18 g	200 Hz	17°	-8°
	8 g	200 Hz	29°	15°
	2 g	200 Hz	45°	5°
	8 g	100 Hz	37°/23°	27°/7°
	2 g	100 Hz	43°/42°	22°/4°
Tested	2 g	100 Hz	47°	23°

$$y(x) = Ax^3 + Bx^2 + Cx + D \tag{4}$$

$$A = \frac{y''(x_i) - y''(x_{i+1})}{6 * h} \tag{5}$$

$$B = \frac{y''(x_i)}{2} \tag{6}$$

$$C = \frac{y(x_{i+1}) - y(x_i)}{h} - \frac{h}{6} * \left(y''(x_{i+1}) - y''(x_i)\right) \tag{7}$$

$$D = y(x_i) \tag{8}$$

IV. CONCLUSION

Proposed device orientation estimation is shown to be good enough for driving style characterization. A standard deviation of 1.67° is acceptable in driving style characterization and crash detection. Regular vehicle dynamics is usually within a range of 2g and it is not sufficient for proper crash detection. It is found that 8g is a sufficient accelerometer dynamic range for crash detection. Cubic interpolation of saturated sensor data further improved crash detection. PDOF information is poorly recovered if crash is not recorded in full range no matter if the sampling rate is increased.

For proper driving style characterization and ACN detection with PDOF estimation with one device it is recommended to use two accelerometer sensors. A low dynamic range accelerometer with high sensitivity should be used for driving style characterization and device kinematic alignment and a high dynamic range accelerometer should be used for ACN detection and PDOF estimation.

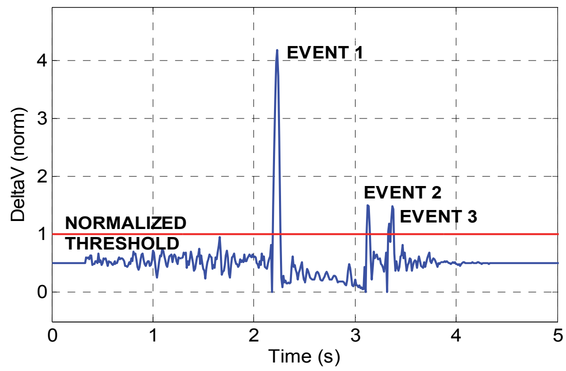

Fig. 12. Cubic approximation partly recovers delta-V.

REFERENCES

[1] R. M. Rogers, "Applied mathematics in integrated navigation systems," 2nd ed., *Rogers Engineering and Associates*, *AIAA*, pp. 18–19, 2003.

[2] M. Park and Y. Gao, "Error and Performance Analysis of MEMS-based Inertial Sensors with a Low-cost GPS Receiver," *Sensors 2008*, pp. 2240-2261, March 29, 2008.

[3] G. Dissanayake, S. Sukkarieh, E. Nebot, and H. Durrant-Whyte, "The aiding of a low-cost strapdown inertial measurement unit using vehicle model constraints for land vehicle applications," *IEEE Trans. On Robotics and Automation*, vol. 17, pp. 733, Oct. 2001.

[4] A. O. Salycheva and M. E. Cannon, "Kinematics Azimuth Alignment of INS using GPS Velocity Information," *Proc. of NTM Conf.*, San Diego, CA, pp. 3, January 26-28, 2004.

[5] P. Davidson, M. A. Vazquez, and R. Piche, "Uninterrupted portable car navigation system using GPS, map and inertial sensors data," *IEEE 13th Int. Symp. on Consumer Electronics*, pp. 2, 2009.

[6] D. Gebre-Egziabher, G. H. Elkaim, J. D. Powell, and B. W. Parkinson, "A Non-Linear, Two-Step Estimation Algorithm for Calibrating Solid-State Strapdown Magnetometers," *Proceedings of the International Conference on Integrated Navigation Systems*, St. Petersburg, Russia, May 2001.

[7] V. Renaudin, M. H. Afzal, and G. Lachapelle, "Complete Triaxis Magnetometer Calibration in the Magnetic Domain," *Journal of Sensors*, vol. 2010, Article ID 967245, Oct. 26, 2010.

[8] M. Huang, *Vehicle Crash Mechanics*, CRC Press, New York, 2002.

[9] U.S. Fed. Register, vol. 76, no. 151, Aug. 5, 2011.